RESEARCH PORTAL CENTRAL

Journal of Bio-Med and Clinical Research

OPEN ACCESS

Research Article

New Reproduction Numbers for Epidemics with the Hidden Cases, Re-Infections, and Newborns

Igor Nesteruk[1]*

1. Institute of Hydromechanics, National Academy of Sciences of Ukraine, Kyiv, Ukraine. Isaac Newton Institute for Mathematical Sciences, Cambridge, UK.

How to cite this article: I. Nesteruk. (2026). New Reproduction Numbers for Epidemics with the Hidden Cases, Re-Infections, and Newborns. *Journal of Bio-Med and Clinical Research*. *RPC Publishers*. 3(1); DOI: https://www.doi.org/rpc/2026/rpc.jbmcr/00534

Address for correspondence: Igor Nesteruk, Institute of Hydromechanics, National Academy of Sciences of Ukraine, Kyiv, Ukraine. Isaac Newton Institute for Mathematical Sciences, Cambridge, UK.
Email: inesteruk@yahoo.com

Submitted: February 04, 2026
Approved: February 28, 2026
Published: March28, 2026

Abstract

Real-time assessments of reproduction numbers are crucial for timely responses to the changes in epidemic dynamics. Known effective reproduction numbers Rt are based on registered (visible) cases, despite that the asymptomatic and unregistered patients occur in all epidemics and need to be corrected to take into account the number of hidden cases. Since the newborns and re-infections significantly affect the dynamics of epidemics, they should also be taken into account in the calculations of Rt and for the recently proposed reproduction rates - the ratios of the real numbers of infectious persons (hidden and registered) at different moments of time. The numbers of cases generated by the symptomatic and asymptomatic patients were introduced, estimated using a novel mathematical model, and compared with the results of a classical SIR (Susceptible-Infectious-Removed) model for the COVID-19 pandemic dynamics in Austria. Reproduction rates R_t were estimated with the use of the visible accumulated numbers of COVID-19 cases in Austria and Tanzania (including the real-time approach). The proposed methods for calculating the reproduction numbers may better reflect the COVID-19 pandemic dynamics than the results listed by John Hopkins University.

Keywords: reproduction numbers; mathematical modeling of infectious diseases; SIR model; COVID-19 pandemic; COVID-19 in Austria; COVID-19 in Tanzania; real-time estimations

Introduction

The effective reproduction number (or reproduction rate) Rt corresponds to the average number of people infected by one person [1, 2]. The known methods of its estimation are based on the registered (visible) cases V(v) [1-9]. Since the real number of cases V can be higher due to the asymptomatic and unregistered patients [10-17], new reproduction numbers must be introduced. It is also necessary to take into account the influence of re-infections [18-21] and newborns [22, 23]. In particular, the new reproduction numbers - the ratios of the real numbers of infectious persons at different moments of time t – were proposed in [24].

In this study, we will generalize the known effective reproduction numbers Rt in order to take into account the unregistered cases and discuss the methods of their estimation with the use of a novel mathematical model [23]. Numerical results for the COVID-19 pandemic in Austria will be presented. The number of cases generated by the symptomatic and asymptomatic patients will be estimated and compared with the results of the classical SIR (Susceptible-Infectious-Removed) model [8,9] and calculations of the effective reproduction number Rt based on the method proposed in [5] and listed in [25].

The new reproduction numbers R_τ (introduced in [24]) will be estimated with the use of visible accumulated numbers of COVID-19 cases in Austria and Tanzania listed in [25]. Corresponding values will be compared with the effective reproduction numbers Rt reported in [25] and calculated using the recommendations of the Robert Koch Institute (RKI) [11].

The real-time assessments of the reproduction rates are crucial for the timely responses to changes in epidemic dynamics [1-7]. The new methods for the real-time calculations of R_τ will be proposed and the results will be compared with the daily numbers of COVID-19 cases registered in Austria in 2020.

In Section 2.1 we will introduce the new effective reproduction numbers showing the numbers of visible and hidden patients infected by one person (symptomatic or asymptomatic) and present formulas for their estimation with the use of a novel model [23]. In Section 2.2 we will show that the new reproduction rates R_τ [24] can be estimated as the ratios of daily cases at different moments of time [24] even when newborns and re-infections are taken into account. A new 7-day smoothing with the use of weighing coefficients will be proposed. In Section 3.1 the new effective reproduction numbers will be calculated for the COVID-19 pandemic in Austria. In Section 3.2, the different reproduction rates and the methods of their calculations will be compared.

Materials and Methods

Effective Reproduction Numbers for the Visible and Hidden Epidemic Dynamics

The effective reproduction number Rt(t) shows the average number of people infected by one person [1, 2]. Since these infections can be visible (registered) with the accumulated numbers of cases V(v) and asymptomatic (hidden and unregistered, $V^{(h)}$) ones, we will use the novel mathematical model (1)- (5), [23].

$$\frac{dS}{dt} = \mu_i - \alpha_i S(I^{(v)} + I^{(h)}) + \delta_i^{(v)} R^{(v)} + \delta_i^{(h)} R^{(h)}, \quad (1)$$

$$\frac{dI^{(v)}}{dt} = \frac{\alpha_i}{\beta_i} S(I^{(v)} + I^{(h)}) - \rho_i^{(v)} I^{(v)}, \quad (2)$$

$$\frac{dI^{(h)}}{dt} = \frac{(\beta_i - 1)\alpha_i}{\beta_i} S(I^{(v)} + I^{(h)}) - \rho_i^{(h)} I^{(h)}, \quad (3)$$

$$\frac{dR^{(v)}}{dt} = \rho_i^{(v)} I^{(v)} - \delta_i^{(v)} R^{(v)}, \quad (4)$$

$$\frac{dR^{(h)}}{dt} = \rho_i^{(h)} I^{(h)} - \delta_i^{(h)} R^{(h)}. \quad (5)$$

with the compartment of infectious personsI(t) separated into the visible (registered) $I^{(v)}$ and hidden $I^{(h)}$ (invisible/asymptomatic and unregistered) parts ($I=I^{(v)}+I^{(h)}$, see eqs. (1)-(5)). The visibility coefficient is the ratio of total infections to the visible ones. This coefficient $\beta_i \geq 1$ was estimated in [14,15] using registered COVID-19 cases. It is also related to the percentage of invisible spreaders [26] and incidence reporting rate [27]. The value corresponds to the fully visible epidemic. The compartment of removed persons R(t) is also divided into the visible (registered) and hidden parts $R = R^{(v)} + R^{(h)}$ with the removing rates $\rho_i^{(v)} I^{(v)}$ and $\rho_i^{(h)} I^{(h)}$, respectively (see eqs. (4) and (5)). We suppose the waning immunity rates to be proportional to the number of the removed persons $\delta_i^{(v)} R^{(v)}$ and $\delta_i^{(h)} R^{(h)}$, [23]. Corresponding terms appear in eqs. (4) and (5) with a minus sign and in eq. (1) with a plus sign. Due to newborns, the number of susceptible persons S(t) increases at the constant rate μ_i (see eq. (1)). The infection, removal and waning immunity rates (α_i, $\rho_i^{(v)}$, $\rho_i^{(h)}$, $\delta_i^{(v)}$, $\delta_i^{(h)}$), the visibility coefficient β_i and the increasing rate of the susceptible persons μ_i are supposed to be constant for every epidemic wave, i.e., for the time periods: $t_i^* \leq t \leq t_{i+1}^*, i = 1,2,3,\ldots$.

Let us introduce two effective reproduction numbers Rti(v) and Rti(h), showing the numbers of visible and hidden patients, respectively, infected by one person (symptomatic or asymptomatic). With the use of total numbers of infectious $I = I^{(v)} + I^{(h)}$ (the sum of visible and hidden ones) and average durations of spreading the infection $1/\rho_i^{(v)}$ and $1/\rho_i^{(h)}$ for the visible and asymptomatic patients during the i-th epidemic wave (corresponding removal rates $\rho_i^{(v)}$ and $\rho_i^{(h)}$ can be different, see eqs. (1), (4) and (5)), the following formulae can be obtained:

$$R_{ti}^{(v)}(t) \approx \frac{1}{\rho_i^{(v)} I(t)} \frac{dV^{(v)}(t)}{dt} \quad (6)$$

$$R_{ti}^{(h)}(t) \approx \frac{1}{\rho_i^{(h)} I(t)} \frac{dV^{(h)}(t)}{dt}. \quad (7)$$

Since new infections (derivatives in eq. (6) and (7)) are appearing according to the visibility coefficient $\beta_i \geq 1$ and the infection rate α_i:

$$\frac{dV^{(v)}}{dt} = \frac{\alpha_i}{\beta_i} SI, \quad (8)$$

$$\frac{dV^{(h)}}{dt} = \frac{(\beta_i - 1)\alpha_i}{\beta_i} SI, \quad (9)$$

eqs. (6)-(9) yield:

$$R_{ti}^{(v)}(t) \approx \frac{\alpha_i}{\beta_i \rho_i^{(v)}} S(t), \tag{10}$$

$$R_{ti}^{(h)}(t) \approx \frac{(\beta_i - 1)\alpha_i}{\beta_i \rho_i^{(h)}} S(t) \ , \tag{11}$$

For the fully visible epidemic ($\beta_i = 1$), eq. (10) coincide with one obtained in [8] and is in good agreement (see [9]) with the Robert Koch Institute (RKI) recommendations to calculate the reproduction number for the COVID-19 pandemic as "the ratio of new infections in two consecutive time periods each consisting of 4 days", [11]. In terms of the smoothed accumulated numbers of visible cases [8, 28]

$$\bar{V}_j^{(v)} = \frac{1}{7} \sum_{k=j-3}^{k=j+3} V_k^{(v)}; \ k \geq 1; k \leq n \ . \tag{12}$$

the RKI rule can be written as follows, [9]:

$$R_t(t_j) = \frac{\bar{V}_{j+4}^{(v)} - \bar{V}_j^{(v)}}{\bar{V}_j^{(v)} - \bar{V}_{j-4}^{(v)}} \tag{13}$$

The effective reproduction number R_{ti} representing the total number of patients (registered and hidden) infected by one person is the sum of (10) and (11):

$$R_{ti}(t) = R_{ti}^{(v)}(t) + R_{ti}^{(h)}(t) = \frac{\alpha_i S(t)}{\beta_i} \left[\frac{1}{\rho_i^{(v)}} + \frac{(\beta_i - 1)}{\rho_i^{(h)}} \right]. \tag{14}$$

If the removal rates for the symptomatic and asymptomatic patients are equal $\rho_i^{(v)} = \rho_i^{(h)} = \rho_i$, eq. (14) does not depend on the visibility coefficient and coincides with one obtained in [8]:

$$R_{ti}(t) == \frac{\alpha_i S(t)}{\rho_i} \tag{15}$$

Reproduction Numbers for Epidemics with Re-infections and Newborns

A new reproduction number

$$R_\tau(t) \equiv \frac{I(t)}{I(t-\tau)} \tag{16}$$

was proposed in [24] to indicate the rate of increasing (decreasing when $R_\tau(t) < 1$) the real number of infectious persons (symptomatic and asymptomatic) during time τ and estimated for the case $\mu_i = \delta_i^{(v)} = \delta_i^{(h)} = 0$. To take into account the newborns and re-infections, let us use relationship (8) in eq. (16). Then

$$R_\tau(t) = \frac{\dot{V}^{(v)}(t) S(t-\tau)}{\dot{V}^{(v)}(t-\tau) S(t)} \tag{17}$$

$$\dot{V}^{(v)}(t) \equiv \frac{dV^{(v)}}{dt} \tag{18}$$

Reproduction numbers in formulae (10), (11), (14)-(17) can be calculated by a numerical integration of set (1)-(5) using the initial conditions listed in [23]. To identify the values of 13 unknown parameters, the least squares method can be used [23, 29]. Usually, the number of susceptible persons S is very large [8, 14- 16, 23, 27] and $S(t-\tau)/S(t) \approx 1$ for small enough values of τ . Then eq. (17) yields

$$R_\tau(t) \approx \frac{\dot{V}^{(v)}(t)}{\dot{V}^{(v)}(t-\tau)} \tag{19}$$

Formula (19) demonstrates that the new reproduction number $R_\tau(t)$ does not depend on the model parameters and can be approximately estimated with the use of daily, weekly, or monthly (according to the unit of time) numbers of the new visible cases. In particular, the following formula can be used, [30]:

$$\dot{V}_j^{(v)} \approx 0.5\left(\frac{V_{j+1}^{(v)}-V_j^{(v)}}{t_{j+1}-t_j}+\frac{V_j^{(v)}-V_{j-1}^{(v)}}{t_j-t_{j-1}}\right) \qquad (20)$$

Where $V_j^{(v)}$, $j=1,2,...,n$ are the accumulated numbers of the visible cases registered at moments tj. A parabolic interpolation yields the following estimation of the daily, weekly, or monthly numbers of new visible cases:

$$\dot{V}_j^{(v)} \approx \frac{V_{j-1}^{(v)}(t_{j-2}-t_j)^2-V_{j-2}^{(v)}(t_{j-1}-t_j)^2-V_j^{(v)}\left[(t_{j-2}-t_j)^2-(t_{j-1}-t_j)^2\right]}{(t_{j-1}-t_j)(t_{j-2}-t_j)(t_{j-2}-t_{j-1})} \qquad (21)$$

which does not contain unknown results of future observations and can be used instead (20) for the real-time estimations. Usually, the daily characteristics are very random (e.g., for the COVID-19 pandemic, [25]), show some weekly periodicity and need smoothing [8, 9, 24, 25, 28]. In particular, the smoothed accumulated numbers of cases (12) can be used. The real-time estimations of the reproduction numbers (17) at the moment $t=t_j$ do not allow using unknown results of future observations ($V_k^{(v)}, k>j$) and eqs. (12), (13), and (20). To estimate derivatives in formula (19), the smoothed daily numbers of new cases, calculated with the use of the previous observations only, can be applied. Since the observations obtained closer to the moment $t=t_j$ have a stronger impact on the trends, some weighing coefficients and the following values:

$$\tilde{V}_k^{(v)} = q^{|j-k|}V_k^{(v)};\ 1\le j\le n; 1\le k\le n; q\le 1\ , \qquad (22)$$

can be used in 7-days smoothing:

$$\tilde{V}_j^{(v)} = \frac{1}{1+q+q^2+q^3+q^4+q^5+q^6}\sum_{k=j-6}^{k=j}\tilde{V}_k^{(v)};\ 1\le k\le n\ , \qquad (23)$$

The value of the parameter q has to be adjusted for every particular case. For example, the value q=1 was used in the John Hopkins University (JHU) datasets to calculate the smoothed numbers of daily COVID-19 cases [25].

Results and Discussions

Calculations of Effective Reproduction Numbers for the COVID-19 Pandemic in Austria

Fig. 1 represents JHU datasets [25] (version corresponding to 11 December 2023) for the number of accumulated (AC, blue "crosses") and daily (DC, smoothed, black "crosses") cases registered in Austria in 2020 and the results of calculations of the effective reproduction number Rt(t) (according to [5], for a fully visible epidemic, red "crosses"). To investigate the influence of hidden cases, the set of differential equations (1)-(5) was integrated numerically with the use of the initial conditions listed in [23] and the fourth order Runge-Kutta method [31]. The value of the time step was adjusted to have accuracy 0.1%. No method of least squares was applied to detect the optimal values of the parameters. We have used only parameter sets that provide some similarity to the observed AC and DC figures registered in April 2020. The solid black curve corresponds to the visible (registered) daily numbers of COVID-19 cases (eq. (8)); the solid blue curve represents the theoretical number of accumulated cases (the integral of (8)) for the following values of parameters:
α_i =1.924971e-05 day^{-1}; $\rho_i^{(v)}$ =0.92365 day^{-1}; $\rho_i^{(h)}$ =0.97226 day^{-1}; $\delta_i^{(v)}=\delta_i^{(h)}$ =0.0202 day^{-1}; μ_i =31.1 day^{-1}; β_i =1.5. The green, magenta, and solid red curves show the effective reproduction numbers (visible, eq. (10); hidden, eq. (11), and total, eq. (14)).

The dashed curves in Fig. 1 correspond to the fully visible epidemic β_i =1; μ_i =0; $\delta_i^{(v)}=\delta_i^{(h)}$ =0; $\rho_i^{(v)}$ =0.92365 day-1, which can be simulated with the use of the classical SIR model [8, 22, 28, 32-35]. The black line yields the theoretical estimation of the daily numbers of cases (eq. (8)); blue – the accumulated number of cases; red – the reproduction number (10). According to the classical SIR model, S(t) values and the reproduction number decrease monotonously with time (see eq. (1) at $\mu_i=\delta_i^{(v)}=\delta_i^{(h)}$ =0, eq. (10) and the dashed red curve in Fig. 1). When the re-infections and newborns are taken into account, the oscillations in the reproduction numbers are possible (see solid magenta, green and red curves) In particular, the total reproduction number (eq. (14) and the red solid line) several times reached the critical value 1.0. The method proposed in [5] (see red "crosses" in Fig.1) yields the much higher magnitude of the oscillations, but the moments of the time, corresponding to the critical values of the reproduction number were very close until mid-June 2020 (compare with the solid red line). Probably, the coincidence can be increased with the use of optimal parameter sets corresponding to the later epidemic periods in (1)-(5).

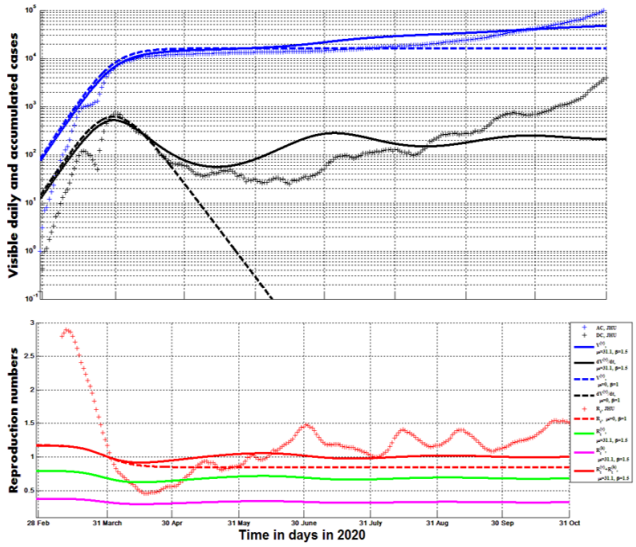

Figure 1: The COVID-19 pandemic dynamics in Austria in 2020. Registered daily and accumulated numbers of cases and calculations of the reproduction numbers.

Blue and black "crosses" represent the visible (registered) accumulated numbers of cases AC and the smoothed daily numbers of new cases DC, respectively, [25]. Red crosses correspond to the calculations of the effective reproduction number by the method proposed in [5] and listed in [25]. Curves show the results of the numerical integration of (1)-(5) at different values of parameters: blue-the visible accumulated number of case $V^{(v)}$; black – the visible daily number of cases $dV^{(v)}/dt$; magenta - the hidden reproduction number $R_{ti}^{(h)}(t)$, eq. (11); green – the visible reproduction number $R_{ti}^{(v)}(t)$, eq. (10); red - the total reproduction number $R_{ti}(t)$, eq. (14).

Comparisons of Different Reproduction Rates and Methods of Their Calculations

In Fig. 2, the results of calculations of the effective reproduction number Rt(t) (according to [5], for the fully visible COVID-19 epidemic in Austria, red "crosses", JHU dataset [25]) are compared with the RKI method (eqs. (12) and (13), the magenta curve). The values shown by red crosses ([5, 25]) diminished almost monotonously until mid-April 2020 and did not reflect the local minimum and the huge increase in the smoothed daily numbers of new cases DC (calculated by using the JHU dataset in eq. (12) and substituting into formula (20), the black curve). In comparison, the RKI method and the calculations of (blue and brown curves) reflect these changes in the epidemic dynamics, yielding the huge increase of reproduction rates. The values (19) at τ =1day calculated by putting the smoothed values (12) into (20) (the blue curve) start to increase simultaneously with DC. When the smoothed DC values listed by JHU are used in (19) (the brown curve), some delay occurs (compare with the black and blue lines).

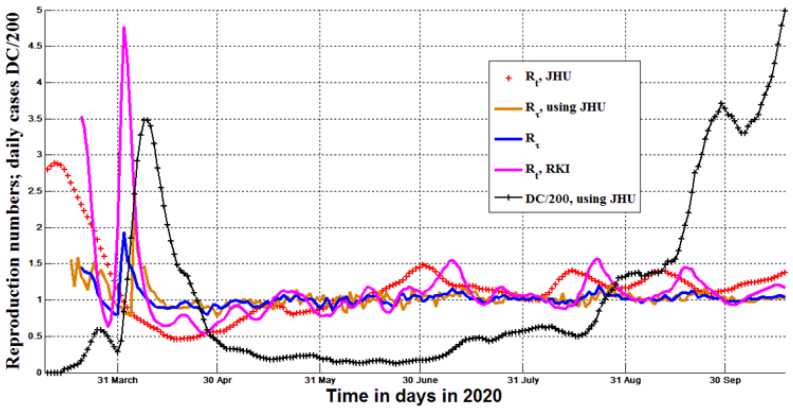

Figure 2: Reproduction rates and the smoothed daily number of COVID-19 cases in Austria in 2020.

The black curve represents the visible (registered) daily number of cases DC smoothed by using the accumulated numbers $V_j^{(v)}$ listed in the JHU dataset [25], eqs. (12) and (20). Red "crosses" correspond to the calculations of the effective reproduction number Rt by the real-time method proposed in [5] (the results are listed in [25]). The magenta line represents

Rt values calculated by the RKI method (eqs. (12), (19), and (20)). Blue and brown curves show calculations of $R_\tau(t)$ (eq. (19), τ =1 day). The brown one was obtained using the smoothed DC values listed by JHU [25]; blue - by putting the smoothed values (12) into (20).

In Fig. 3, the results of calculations of the reproduction rates Rt(t) and are compared with the COVID-19 pandemic dynamics in Tanzania (the accumulated number of cases AC is shown by blue "triangles"). Red "crosses" correspond to the calculations of the effective reproduction number Rt by the real-time method proposed in [5] (the figures are listed in [25]). These values diminished monotonously and did not reflect the huge increase in the numbers of cases registered in April 2020 (in comparison with the Rt values calculated by the RKI method (the magenta curve)). It must be noted that all Rt figures listed by JHU [25] for Tanzania are subcritical (Rt <1), while for an epidemic outbreak (or a new wave) to occur, we need to have Rt >1. Blue and black curves show the calculations of $R_\tau(t)$ (eq. (19) at τ =1 day). The black one was obtained using the smoothed DC values listed by JHU [25]; blue - by putting the smoothed values (12) into (20). All curves in Fig.3 show some supercritical values and reflect the increase in the number of cases. The black line is more chaotic and reflects the increase in the number of cases with some delay (in comparison with the blue one).

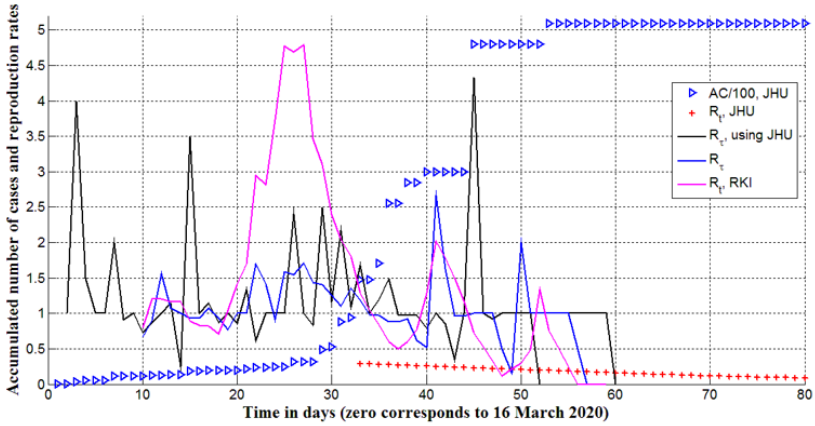

Figure 3: Reproduction rates and the accumulated number of COVID-19 cases in Tanzania in 2020.

The blue "triangles" represent the visible (registered) accumulated number of cases AC divided by 100 (according to the JHU dataset [25]). Red "crosses" correspond to the calculations of the effective reproduction number Rt by the method proposed in [5] and listed in [25]. The magenta line represents Rt values calculated by the RKI method (eqs. (12), (19), and (20)). Blue and black curves show calculations of $R_\tau(t)$ (eq. (19), τ =1 day). The black one was obtained using the smoothed DC values listed by JHU [25]; the blue curve - by putting the smoothed values (12) into (20).

Thus, some estimations of Rt fail to reflect changes in epidemic dynamics (compare red "crosses" with DC and AC values in Figs. 2 and 3). In comparison, the presented calculations of $R_\tau(t)$ demonstrated increase and supercritical values for the periods, when the daily number of cases increased. Unfortunately, the real-time estimations of $R_\tau(t)$ show some time delay (compare the brown and black curves with the blue one in Figs. 2 and 3). This fact limits the applicability of the real-time approaches for the effective control of the epidemic dynamics. Nevertheless, the delay can be diminished with the use of weighing coefficients (see eq. (22) and (23)).

In Fig. 4, different methods of calculations of the reproduction rate $R_\tau(t)$ are presented and compared with the daily numbers of COVID-19 cases in Austria, smoothed with the use of AC values listed in [25], eqs. (12) and (20) and divided by 500. Other curves show calculations of $R_\tau(t)$ (eq. (19) at =1 day). Blue one was calculated by putting the values (12) into (20) (the median (not real-time) smoothing). Red, magenta, and green curves correspond to the real-time estimations using smoothed DC values according to the JHU dataset [25] (red); obtained by putting the smoothed values (23) into (21) at q=1 (magenta) and q=0.5 (green).

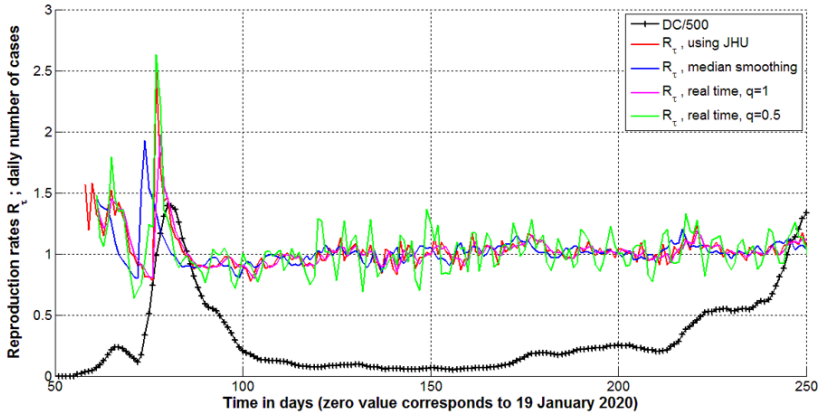

Figure 4: Reproduction rates $R_\tau(t)$ and the smoothed daily number of COVID-19 cases in Austria in 2020.

The black curve represents the visible (registered) daily number of cases DC smoothed using the accumulated numbers $V_j^{(v)}$ listed in the JHU dataset [25], eqs. (12) and (20) and divided by 500. Other curves show the calculations of $R_\tau(t)$ (eq. (19), τ =1 day). Blue one was calculated by putting the values (12) into (20) (the median (not real-time) smoothing). Red, magenta, and green curves correspond to the real-time estimations using the smoothed DC values according to the JHU dataset [25] (red); obtained by putting the smoothed values (23) into (21) at q=1 (magenta) and q=0.5 (green).

Red and green curves are very close, illustrating the fact that eq. (19) allows us to calculate the reproduction rates $R_\tau(t)$ using the smoothed DC values for the fixed and previous moments of time or eqs. (21)-(23) at q=1. The value q=0.5 yields more chaotic behavior of $R_\tau(t)$ (green curve), but decreases the delay between the changes $R_\tau(t)$ in and the epidemic dynamics. Probably, the value of q can be optimized for every epidemic. For some diseases, only monthly or weekly numbers of new cases are available (e.g., the pertussis epidemic in England, [36]). Then there is no need to use smoothing, and the real-time estimations of $R_\tau(t)$ can be obtained using (19) and (21).

Conclusions

The impact of newborns and re-infections on the visible and hidden epidemic dynamics and the reproduction rates was taken into account with the use of a novel mathematical model. The known reproduction rate Rt was generalized to show the number of cases generated by symptomatic and asymptomatic patients, which were calculated for the COVID-19 pandemic in Austria in 2020. When the re-infections and newborns are taken into account, the oscillations in reproduction numbers are possible. In particular, the total reproduction number (the sum of the number of cases generated by symptomatic and asymptomatic patients) reached the critical value 1.0 several times.

The methods for calculations of the recently proposed reproduction rates R_τ - the ratios of the real numbers of infectious persons at different moments of time – are presented and estimated with the use of the visible accumulated numbers of COVID-19 cases in Austria and Tanzania (including the real-time approach). The proposed methods for calculating the reproduction numbers may better reflect the COVID-19 pandemic dynamics than the results listed by John Hopkins University.

Unfortunately, the real-time estimations of $R_\tau(t)$ show some time delay. This fact limits the applicability of the real-time approaches for the effective control of the epidemic dynamics. Nevertheless, the delay can be diminished with the use of the weighing coefficients. The topics for further research may be the search for the optimal values of these coefficients and modification of the approach (1)-(5) using SEID and more complicated models.

Declarations

Ethics Approval and Consent to Participate: No humans or human data was used during this study.

Consent for Publication: Not applicable.

Availability of Data and Material

Only open datasets available on Internet and listed in the text were used in this study.

Competing Interests: The author declares no conflict of interests.

Funding: The study has not received any special funding

Authors' Contributions: There is only one author. I.N. has done this study and written the manuscript

Acknowledgements: The author is grateful to the INI-LMS Solidarity Programme at the University of Warwick, UK, and his colleagues - Ulrike Tillmann, James Robinson, Robin Thompson, Matt Keeling, Paul Brown, and Oleksii Rodionov - for their support and valuable information.

References

1. Epidemic theory (effective & basic reproduction numbers, epidemic thresholds) & techniques for analysis of infectious disease data (construction & use of epidemic curves, generation numbers, exceptional reporting & identification of significant clusters). *Faculty of Public Health.*
2. (2020). Effective reproduction number estimation. *R-Bloggers.*
3. An Der Heiden M, O. Hamouda. (2020). Schätzung Der Aktuel-Len Entwicklung Der Sars-Cov-2-Epidemie in Deutsch-Land – Nowcasting. *Epid Bull,* 17:10-15.
4. Cori, Anne, Neil M. Ferguson, Christophe Fraser, Simon Cauchemez. (2013). A New Framework and Software to Estimate Time-Varying Reproduction Numbers During Epidemics. *American Journal of Epidemiology,* 178(9):1505-1512.
5. Arroyo-Marioli F, Bullano F, Kucinskas S, Rondón-Moreno C. (2021). Tracking R of COVID-19: A new real-time estimation using the Kalman filter. *Plos One,* 16(1):e0244474.
6. R.N. Thompson, J.E. Stockwin, R.D. van Gaalen, J.A. Polonsky, Z.N. Kamvar, et al. (2019). Improved inference of time-varying reproduction numbers during infectious disease outbreaks, *Epidemics,* 100356, ISSN 1755-4365.
7. I Ogi-Gittins, WS Hart, J Song, RK Nash, J Polonsky. (2023). A simulation-based approach for estimating the time-dependent reproduction number from temporally aggregated disease incidence time series data. *MedRxiv,* 23295471.
8. Nesteruk I. (2023). Improvement of the software for modeling the dynamics of epidemics and developing a user-friendly interface. *Infectious Disease Modelling,* 8(3): 806-821, ISSN 2468-0427.
9. Nesteruk I, Brown P. (2024): Impact of Ukrainian Refugees on the COVID-19 Pandemic Dynamics after. *Computation,* 12:70.
10. (2024). Slovakia's Second Round of Coronavirus Tests Draws Large Crowds. *COVID-19 Pandemic.*
11. Schreiber P.W, Scheier T, Wolfensberger A. et al. (2023). Parallel dynamics in the yield of universal SARS-CoV-2 admission screening and population incidence. *Sci Rep,* 13:7296 (2023).
12. Fowlkes A.L, Yoon S.K, Lutrick K, Gwynn L, Burns J, et al. (2022). Effectiveness of 2-Dose BNT162b2 (Pfizer BioNTech) mRNA Vaccine in Preventing SARS-CoV-2 Infection Among Children Aged 5-11 Years and Adolescents Aged 12–15 Years -PROTECT Cohort, July 2021–February 2022. MMWR Morb. Mortal. *Wkly. Rep,* 71:422-428.
13. Shang W, Kang L, Cao G, Wang Y, Gao P, Liu J, Liu M. (2022). Percentage of Asymptomatic Infections among SARS-CoV-2 Omicron Variant-Positive Individuals: A Systematic Review and Meta-Analysis. *Vaccines (Basel),* 10(7):1049.
14. Nesteruk I. (2021): Visible and real sizes of new COVID-19 pandemic waves in Ukraine. *Innov Biosyst Bioeng,* 5(2):85-96.
15. Nesteruk I. (2021) Influence of Possible Natural and Artificial Collective Immunity on New COVID-19 Pandemic Waves in Ukraine and Israel. *Exploratory Research and Hypothesis in Medicine.*
16. Nesteruk I. (2025). General SIR model for visible and hidden epidemic dynamics. *Front. Artif. Intell,* 8:1559880.
17. Rodger Craig et al. (2020). Asymptomatic Infection and Transmission of Pertussis in Households: A Systematic Review. *Clin Infect Dis,* 70(1):152-161.
18. COVID-19 Reinfection Data. COVID-19 Data in New York. *New York State.*
19. Guedes A.R, Oliveira M.S, Tavares B.M. et al. (2023). Reinfection rate in a cohort of healthcare workers over 2 years of the COVID-19 pandemic. *Sci Rep,* 13:712.
20. Flacco M E et al. (2022). Risk of SARS-CoV-2 Reinfection 18 Months After Primary Infection: Population-Level Observational Study. Front. Public Health, 02 May 2022. Sec. Infectious Diseases: *Epidemiology and Prevention.*
21. Nesteruk I. (2023). Endemic characteristics of SARS-CoV-2 infection. *Sci Rep,* 13:14841.
22. M. Keeling, P. Rohani. (2008). Modelling Infectious Diseases in Humans and Animals. *Princeton Univ. Press, Princeton, NJ.*
23. Nesteruk, I. (2025). How Re-Infections and Newborns Can Impact Visible and Hidden Epidemic Dynamics? *Computation,* 13:113.
24. Nesteruk I. (2025). New reproduction numbers for the visible and real epidemic dynamics. *MedRxiv.*
25. (2023). COVID-19 Data Repository by the Center for Systems Science and Engineering (CSSE) at Johns Hopkins University (JHU).

26. Wu C, Xu C, Mao F, Xu X, Zhang C. (2022). The impact of invisible-spreaders on COVID-19 transmission and work resumption. *PLOS ONE,* 17(1):e0252994.
27. Smirnova A, Baroonian M. (2024). Reconstruction of incidence reporting rate for SARS-CoV-2 Delta variant of COVID-19 pandemic in the US. *Infectious Disease Modelling,* 9(1):70-83.
28. Nesteruk I. (2021). COVID19 pandemic dynamics. *Springer Nature.*
29. Plackett R.L. (1972). The discovery of the method of least squares (PDF). *Biometrika,* 59(2):239-251.
30. Nesteruk, I. (2024): Mathematical simulations of the pertussis epidemic in England. International Workshop Prof IT AI 2024, *Cambridge, MA, USA,* 25-27.
31. Martha L. Abell, James P. Braselton. (2014). Chapter 6 - Systems of Differential Equations, Editor(s): Martha L. Abell, James P. Braselton, Introductory Differential Equations (Fourth Edition), *Academic Press,* 277-364, ISBN 9780124172197.
32. Kermack WO, McKendrick AG. (1927). A Contribution to the mathematical theory of epidemics. *J Royal Stat Soc Ser A,* 115:700-721.
33. Weiss H. (2013). The SIR model and the foundations of public health. *Mat Mat,* 3:1-17.
34. Daley DJ, Gani J. (2005). Epidemic Modeling: An Introduction. New York: *Cambridge University Press.*
35. Alireza Mohammadi, Ievgen Meniailov, Kseniia Bazilevych, Sergey Yakovlev, Dmytro Chumachenko. (2021). Comparative study of linear regression and SIR models of COVID-19 propagation in Ukraine before vaccination. *Radioelectronic and Computer Systems,* 3:5-18.
36. Confirmed cases of pertussis in England by month - GOV.UK (www.gov.uk).